Current Trends in Neurology
Vol. 6, 2012

Original Communication

Specific localizations of cytokines and Parkinson's disease-associated proteins revealed by fluorescence deconvolution microscopy in brain tissues of an LPS treated rat model

Marie-Francoise Doursout[1], Mya C. Schiess[2], Michael S. Schurdell[3], Uzondu Osuagwu[3], Diana M. Hook[3,4], Brian J. Poindexter[3], Diane L. M. Hickson-Bick[3] and Roger J. Bick[3,*]

Departments of [1]Anesthesiology, [2]Neurology, [3]Pathology and [4]Surgery, University of Texas Health Science Center, Houston, Texas, USA

ABSTRACT

This study was performed to examine cytokines and Parkinson's disease (PD) associated proteins in brains of a rat lipopolysaccharide (LPS) model using fluorescence microscopy for quantifying and identifying locations of cytokines and neurodegenerative proteins. Rats were treated with LPS and organs were removed for determinations of nitric oxide (NO) content. Brain was sectioned and fluorescence deconvolution microscopy was used to localize both Parkinson's disease-associated proteins and cytokines. Quantities were determined. NO levels increased in many tissues, including brain. Fluorescence labeling revealed double staining of cells for interleukin-6 and tau protein. Vascular endothelium labeled for both tumor necrosis-alpha (TNF) and ubiquitin. Many immune cells were visible in LPS brains, suggesting an inflammatory episode preceded migration of cytokine producing cells from the circulation and cerebrospinal fluid, initiating a neurodegenerative cascade in susceptible cells, while predisposing them to succumb to subsequent inflammatory episodes. Inflammatory cells and cytokines were seen in perivascular areas, associated with meninges, and concentrated between the olfactory bulb and cortex, indicating the likelihood of specific interactions with specific cells. TNF and glial cell line-derived neurotrophic factor (GDNF) showed a modest, sustained increase, while IL-1β and IL-10 exhibited abrupt, rapid increases, followed by sharp decreases. Results suggest that a gradual decline in neuronal sustainability occurs, with subsequent assaults initiating a protective mode that is overcome, and this gradual decline might describe the long term process of PD, with neurons becoming targeted by pro-inflammatory cytokines, protein aggregations and loss of the ubiquitin-proteasome recycling pathway late in the process.

KEYWORDS: Parkinson's disease, cytokines, neurodegeneration, fluorescence microscopy

INTRODUCTION

There have been numerous reports that Parkinson's disease (PD) is the result of an inflammatory episode or episodes and, as we have hypothesized, leads to sustained detrimental protein aggregations and signaling disruption, either due to one massive event (high cytokine levels), or a sequence of smaller events that are additive over time and result in reduced neuron survival. That is, continuous exposure to toxic

*Corresponding author:
Roger.J.Bick@uth.tmc.edu

compounds such as cytokines, eventually overcome cell protective mechanisms [1, 2, 3].

A cell culture model using glioblastoma cells [4], cells that are both robust and able to synthesize the PD associated proteins tau, alpha-synuclein and ubiquitin, showed that both cytokine and LPS treatments produced protein aggregations [5], which resulted in a loss of cell adhesion and necrotic cell death [6]. Similar protein aggregation findings were seen in brains of LPS-treated rats leading us to hypothesize that the same or similar mechanisms were in place in both models, mechanisms that resulted in the demonstration of cytokine induced protein disruptions that occur in Parkinson's neurodegeneration. There is also strong support for the use of LPS in studies on, and of, the progress of neurodegeneration [7] as expression of iNOS (inducible nitric oxide synthase) and peripheral inflammation following LPS administration has been linked to glial activation and alterations in cell death pathways [8]. Therefore, to further elucidate which particular cell types were associated with cytokine release and to map co-localizations of these inflammation-associated products with specific proteins, brains from LPS treated rats were sectioned and stained with appropriate antibodies, photographed and imaged by deconvolution microscopy with selected fluorescent probes [4, 5] while measuring nitric oxide (NO) levels in multiple tissues to demonstrate that a systemic, inflammatory event had occurred. Levels of iNOS were determined in brain sections as a number of previous reports using mouse models have implicated NOS in both neuron protection and destruction [9, 10, 11, 12] as well as regulations in cardiovascular function through astrocyte-neuron interactions [13]. NOS levels in other organs were also determined as previous reports noted that induction not only occurred in brain tissue, but was a cause of global cell destruction and compromised biochemical signaling, suggesting that other cells and tissues, such as immune cells, might well contribute to the onset of PD and loss, of protective abilities [8, 14].

Many cell types are involved in the development and continuation of PD, but while present treatments are often targeted at replenishing the loss of the neurotransmitter dopamine, the strategy does not take into consideration changes to other cell types and associated structures [11, 12, 15]. Our initial studies involved the treatment of cultured nerve cells with LPS and cytokines in an attempt to mimic *in vivo* inflammatory episodes, and induce protein aggregations and cell death. As protein aggregations did occur in our experiments [4, 5, 6], we utilized an endotoxin LPS rat model and tissue imaging, assuming that similar protein changes would be evident in specific areas of the brain. Similar protein aggregations to those seen in the cell cultures were indeed apparent in the animal tissues and a definite inflammatory component appeared to be intimately involved in the formation of these aggregations. It was therefore deemed that the logical next step would be to examine brain slices of specific areas to identify cytokine content and type, and determine co-localizations of these products in specific cells as well as with PD-associated proteins and tissue structures.

The review by Arai and colleagues [7] states that mechanisms in neurodegeneration are poorly understood; that an inflammatory response is most likely involved in PD progression; that repeated doses of LPS exacerbates motor axon degeneration, similar to our findings with cultured cells [5, 6]; and that LPS can cause a breakdown of the blood-brain barrier and involve other cell types, such as we and others have hypothesized [6, 15].

As inflammation and the innate immune system appear to be involved in PD [16, 17], our LPS model and measurements of iNOS again appear reasonable, as Arai and colleagues also stated, "There is considerable evidence that NO could be pivotal to the pathogenesis of PD" [5, 13].

METHODS

Sectioning and staining of tissues

Adult rat brains (300 g Sprague Dawley; males), from untreated control, saline-injected animals and LPS treated animals (35 mg/kg), were removed, fixed, sectioned and probed with specific antibodies. Tagged secondary antibodies were added to facilitate visualization via deconvolution fluorescence microscopy. Images were acquired in a stepwise section thickness (0.1-0.25 µm) from

the olfactory bulb, cortex, substantia nigra and striatum following the guidelines of Paxinos and Watson [18].

Imaging

Sections were mounted on 25 mm glass cover slips and fluorescently probed for α-synuclein (ab10789-100), ubiquitin (ab7780-50), tau (ab8763-250; Probes from Abcam, Cambridge, MA), interleukin-6 (IL-6), interleukin-10 (IL-10), tumor necrosis factor-alpha (TNF-α) and gamma-interferon (λ-IFN; IL-6 - 500-P73; TNF-α -500-P80; IL-10 - 500-P139h and IL-1-β 500-P80 (antibodies from Peprotech, Rocky Hill, NJ). Tissue was rinsed with cold, 1X PBS followed by fixation with 3.7% formaldehyde (1008B, Tousimis Research Corporation, Rockville, MD). Fixation was stopped by 3 rinses with 1X phosphate buffered saline at room temperature. Tissue was blocked with 10% goat serum and incubated for 1 hr. at 37ºC with antibodies (1:100 to 1:1000 dilution), incubated for 30 min. at 37^{o}C and rinsed 2 to 3 times with 0.05% Tween 20 in 1X PBS (TPBS). Finally, nuclei and F-actin were stained with Phallicidin (Invitrogen, Grand Island, NY, USA) diluted 1:100 in 4',6-diamidino-2-phenylindole (DAPI; A-T rich region binding in DNA) solution. Specimens were mounted onto slides using a drop of Elvanol (DuPont, Wilmington, DE). Fluorescence microscopy and fluorescence intensity measurements were made using pixel counts of labeled proteins, cytokines and NOS as previously described [4] and 3D reconstructions and rotations were performed [19].

NOS and isoforms

Frozen tissues were homogenized at a ratio of 1g per 3-6 ml of buffer. Homogenization was first performed with pestle and mortar and then with an homogenizer in ice + salt cold environment. Homogenization buffer (pH 7.4) was 50 mM 4-(2-hydroxyethyl)-1-piperazineethanesulfonic acid, 100 µM dithiothreitol, 55 µM leupeptin, 100 µg mL^{-1} phenylmethylsulfonyl fluoride, 2 µg mL^{-1} aprotinin, 1.4 µM pepstatin A, and 2.5% glycerol in double-distilled water. The homogenate was centrifuged at 10,000 g for 15 min at 4°C. Supernatants were aliquoted and frozen at -70°C.

Western blot

Concentrations of iNOS, nNOS and nitrotyrosine in collected tissue samples were measured using specific antibodies. Frozen tissue homogenates were thawed on ice and mixed with equal volumes of sample buffer (200 mM Tris-HCl (pH 6.8), 8% sodium dodecyl sulfate, 30% glycerol + 1% β-mercaptoethanol, 0.5% bromophenol blue), then heated at 95°C for 5 to 10 min. Samples were centrifuged and loaded on 8% Tris/glycine/sodium dodecyl sulfate-polyacrylamide gels for fractionation, with predetermined molecular weight standards (Novex Inc., Encinitas, CA). Protein was blotted onto nitrocellulose membranes at 4°C at 30 V and 380 mA for 150 min. After transfer, the membranes were incubated with 5% skim milk in Tris-buffered saline containing 0.05% Tween 20 for 2 h at room temperature [20].

Nitrotyrosine immunoblot

Samples for immunoblot analysis were boiled for 3 min and electrophoresed on 12.5% acrylamide gels. The proteins were electrophoretically transferred to nitrocellulose sheets using a semidry apparatus. The sheets were reacted with a monoclonal mouse anti-nitrotyrosine antibody (Zymed Laboratories, South San Francisco, CA). Immune complexes were detected using peroxidase-labeled goat anti-mouse immunoglobulin G (KPL, Inc., Gaithersburg, MD; 20. Please see Figure 1), as a marker to show that oxidative stress had occurred due to LPS treatment [21].

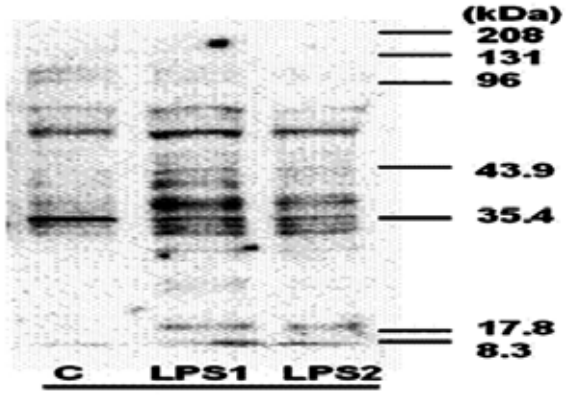

Figure 1. Western blot analysis of nitrotyrosine-containing proteins in lung extracts from control (C) and LPS treated rats (LPS1 and LPS2) at 6 hr.

RESULTS

Figure 2 shows the co-localization of IL-6 and tau in a neuron. It is of interest to note that not all cells in the section demonstrate this co-localization and not all the cells reveal the presence of one or other of these products. Also relevant is the localization of tau (red) to what appears to be the origination point of a dendrite identified with a white arrow in both the 600X mag. and 900X (upper, right panel). An embossed image is included (lower, right panel) to permit a volumetric comparison. To further delineate this 'specificity', Figure 3 shows examples of co-localizations of other products associated with an inflammatory response to specific structures and areas. Panel A is an image of the perivascular 'clustering' of tau following LPS treatment, panel B reveals the co-localization (yellow) of tau with IL-6 (green probe), whereas in panel C the co-localization of ubiquitin and TNF can be seen in arteriole endothelial cells.

As a loss of olfaction has been implicated in the progression of PD, we focused much of our attention on the olfactory bulb. Figure 4 shows 'aggregation' of Tau along the margin of the bulb (Panel A, red areas) and the cortex, while α-synuclein is found in the same location, albeit at a lower concentration (Panel B).

Our data also demonstrate definite trends in increases/decreases of certain cytokines and proteins following LPS treatment (Figure 5). IL-6 levels were reduced 12 hours after LPS treatment, while α-synuclein was a) reduced in overall tissue levels but b) aggregated in specific areas of the olfactory bulb and substantia nigra. In contrast, both γ-interferon and ubiquitin concentrations increased.

Figure 6 demonstrates the localization of specific products to diverse structures and a defined group of cells (positive vs. negative cells) in various brain sections. The upper left panel shows IL-10 along an axon and dendrites, as well as being present in small amounts throughout this tissue. The upper right panel shows IL-1β distributed at a high concentration throughout the tissue on the left side of the panel but with no IL-1β associated with the vasculature; the lower left panel clearly shows the localization of IL-4 to a specific cell population, in a perinuclear pattern, while the lower right panel shows iNOS distributed predominantly around the arteriole.

To show that a systemic inflammatory episode does indeed occur due to LPS injection, we have included some data from a previous publication (Figure 7; [21]) showing that iNOS activity is dramatically increased in many tissues, (here shown 8 hours after administration of 200 μg/kg LPS in the histogram), with accompanying images of the liver to show the massive induction (iNOS) in this organ. Given our experimental protocols, the LPS treatment is obviously more than adequate to initiate an inflammatory episode, intense enough to result in high levels of cytokine synthesis and release, the initiation of cell death pathway, and blood-brain barrier complications.

Multiple co-localizations have been seen in our LPS animal model, a model of infection that has been used successfully in neurodegeneration studies [4, 5, 6]. Image reconstructions were therefore made and 3D models of the stacked sections were generated as previously described [19].

The first image (upper left, Figure 8) demonstrates the specific localizations of Tau (red) and IL-6 (yellow) in a neuron (note dendritic IL-6 after LPS injection; white arrows); the second image (upper right) shows the co-localization of Tau (red) and α-synuclein (yellow) in specific cells along the margin between the olfactory bulb and the cortex (white arrow), while the third image (bottom) demonstrates the co-localization (white arrow) of TNF (red) and ubiquitin (yellow) in the endothelial cells of this vessel in the striatum.

Finally, Figure 9 demonstrates an increase in component GDNF over the first 12 hours following LPS treatment, together with a parallel increase of TNF, possibly suggesting an attempt at cell protection against toxic cytokines.

DISCUSSION

Theodore and co-workers [22] noted in the discussion of their recent paper, "Because it is likely that neuroinflammation is important in the onset *or* progression of human PD, identifying the mechanisms of immune activation in this model may lead to novel therapies for the disease" [23].

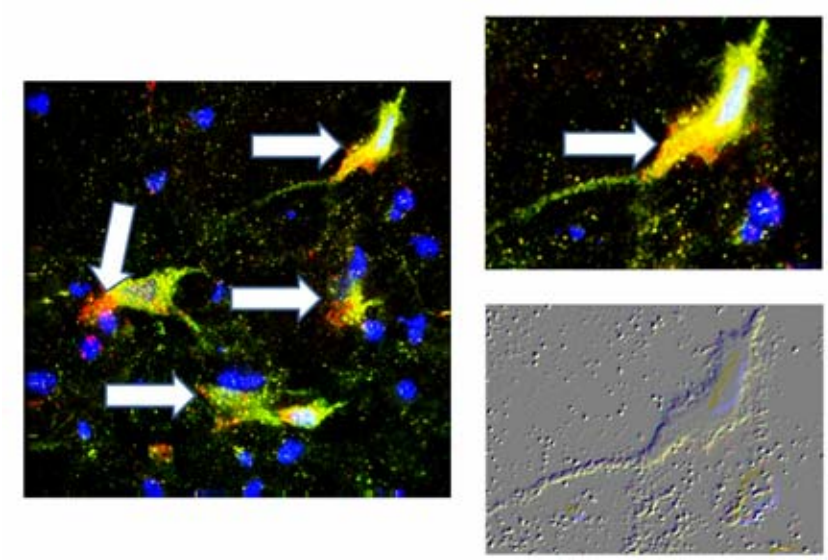

Figure 2. This figure details the specificity of fluorescent labeling in sections of rat cortex. The double labeling in this image at a low (600X; left panel) and high (900X; upper right panel) magnification, shows both IL6 (red) and tau (green) protein (white arrows; yellow color indicates co-localization; nuclei are blue), with the upper right (900X) panel detailing the high concentration of IL6 at one end of the cell (white arrow) where a dendritic extension originates. An embossed rendition is shown (lower right panel) to aid in viewing the cell shape and size. Deconvolution was via 5 iterations.

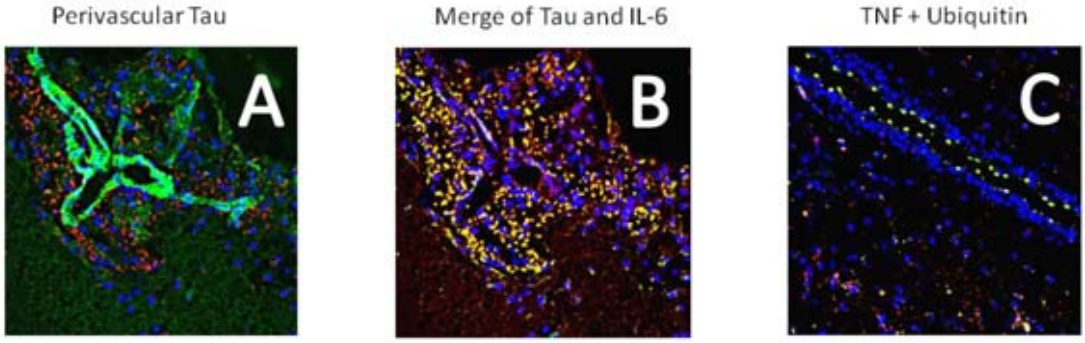

Figure 3. Panel A shows tau distributed around an arteriole, while the image in panel B reveals that the tau marker is co-localized with IL6. Other staining experiments (not shown here) showed that the cells were lymphocytes and macrophages.

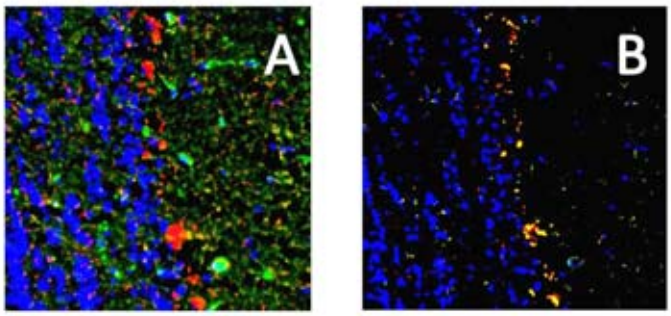

Figure 4. Tau protein (red) is shown demarcating the junction between the olfactory bulb and the cortex (left panel). The right panel shows tagged alpha-synuclein in a similar position.

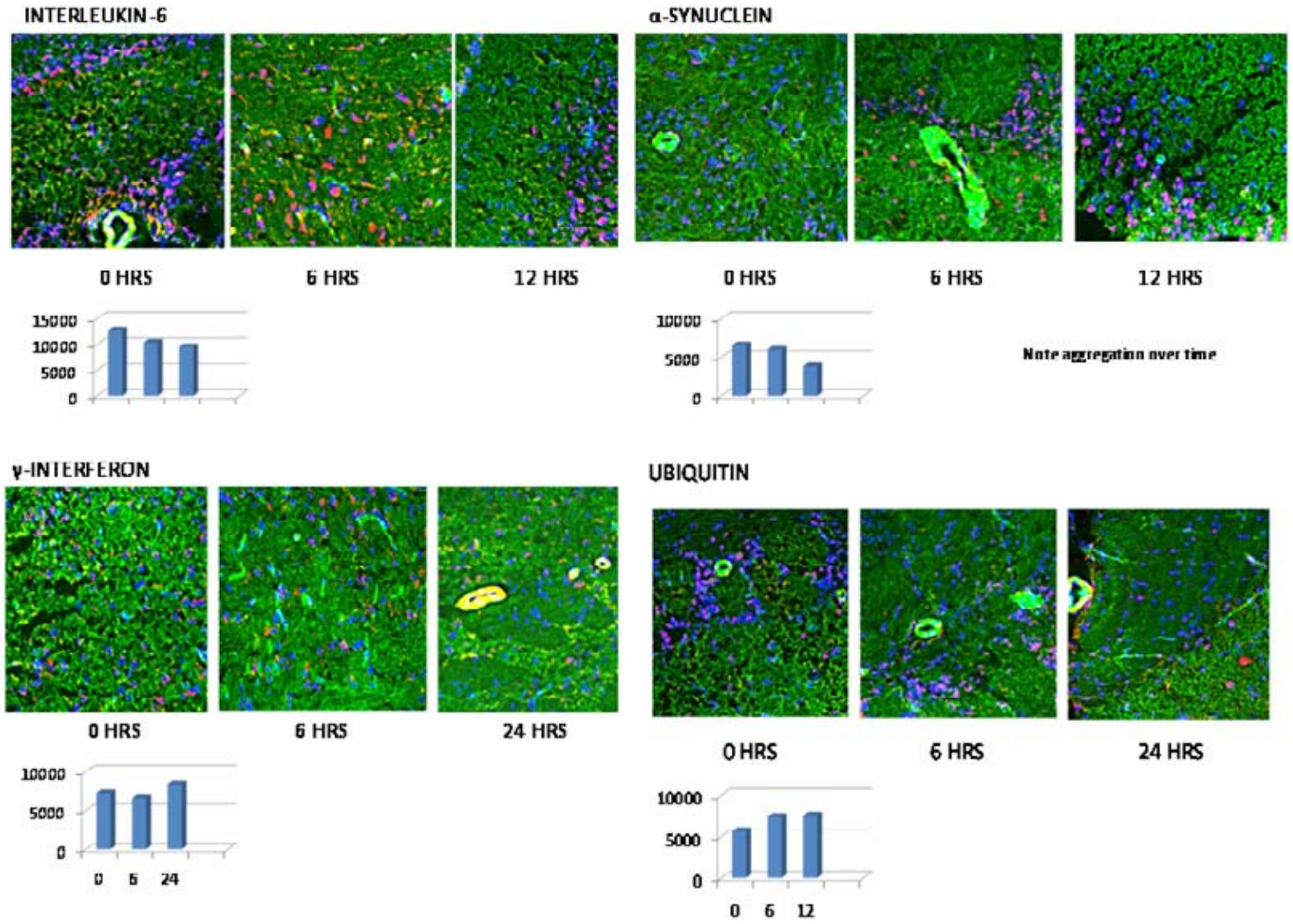

Figure 5. This figure shows a compilation of images to demonstrate increases, decreases and some aggregations of a number of inflammatory and PD-associated compounds/proteins. The accompanying blue bars indicate the trends. Not that both IL6 and alpha synuclein demonstrate a gradual decrease 6 hours after LPS treatment, but there is consolidation and/or aggregation to certain tracts and cells. Gamma-interferon shows a slight increase over time, but a focused or specific distribution was not apparent. Ubiquitin also increased, and aggregations of this product were clearly evident.

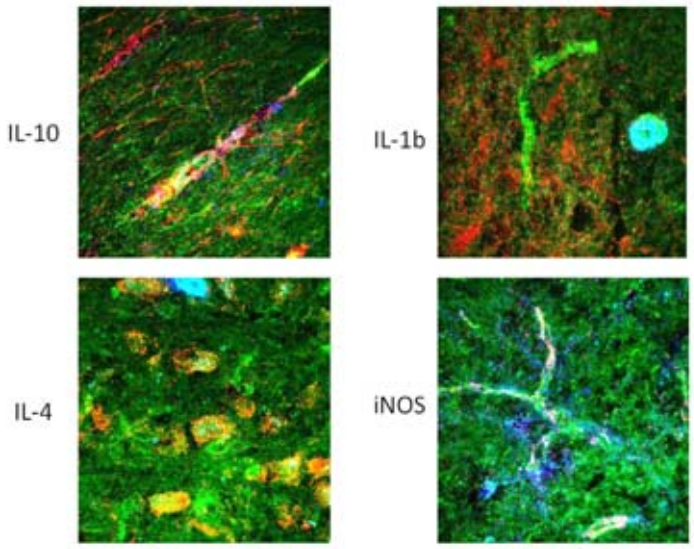

Figure 6. This figures demonstrates particular specific locations of products of interest, such as IL10 along dendrites in panel A, IL-1beta throughout the tissue, but much more concentrated to the left of the image (panel B); Panel C shows IL4 localized to a particular subset of cells, while panel D shows iNOS along vessels (Magnification x900).

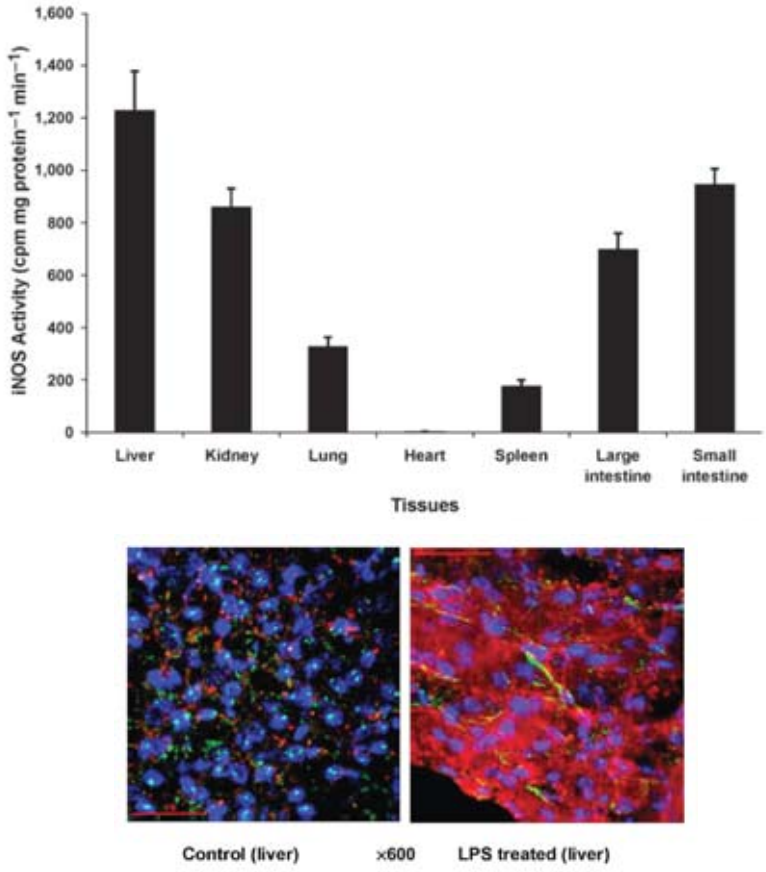

Figure 7. Histogram - iNOS activity recorded at 8 h in various tissues, for example, liver, kidney, lung, heart, spleen, and large and small intestine in pigs challenged with LPS. Bottom images show iNOS recorded by immunofluorescence staining in the liver in control and LPS treated pigs. DAPI (nuclei); green, smooth muscle actin (vasculature); red, iNOS.

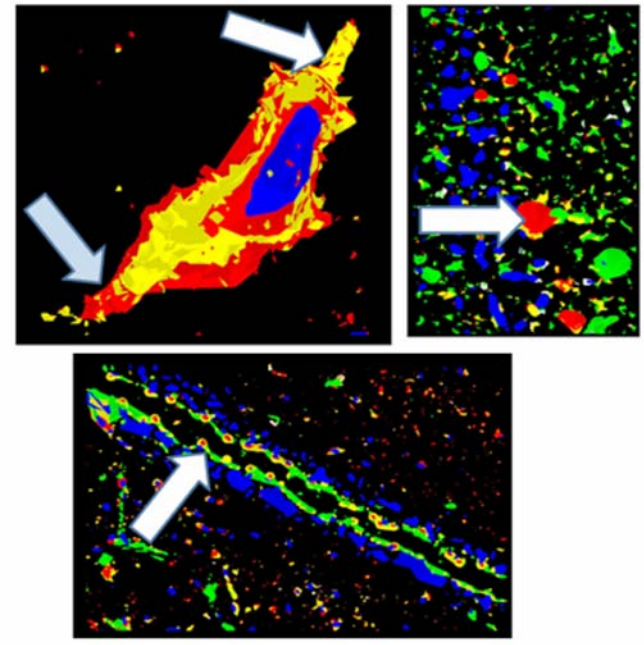

Figure 8. The first image demonstrates specific localizations of Tau (red) and IL6 (yellow) in deconvoluted, stacked, 3D rendition of a neuron (note axonal IL6) from the brain of an LPS treated animal; the second image shows co-localization of Tau (red) and α-synuclein along the margin between the olfactory bulb and the cortex modeled as described above, while the third image demonstrates co-localization of TNF (red) and ubiquitin (yellow) in the endothelial cells of this 3D modeled vessel in the striatum.

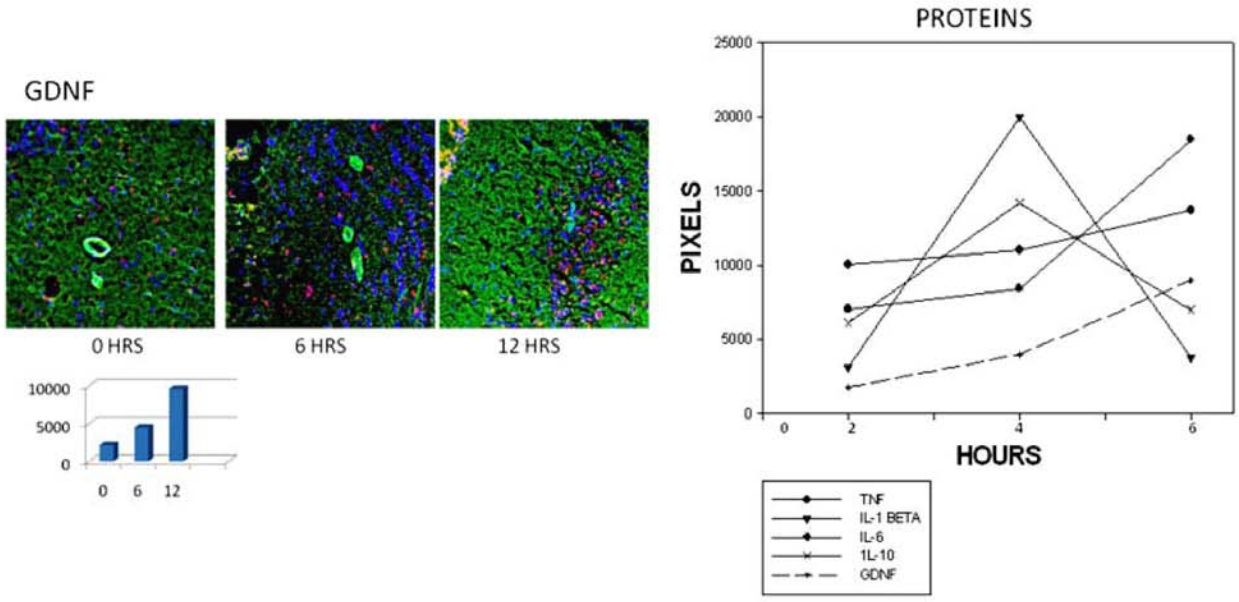

Figure 9. Three images to show increasing fluorescence labeling of GDNF in brains from LPS treated rats over the first 12 hours (Mag. X600; GDNF-red; actin-green; nuclei-blue), together with pixel measurements from a representative experiment measuring cytokine levels to yield an insight into the initiation of a protective pathway.

As a result, our studies have continued along this vein of investigation, in which we hypothesize that certain cells are prone to neurodegeneration, while others are somewhat resilient and resist entering cell death pathways until protective mechanisms are overcome by repeated, inflammatory episodes.

The studies reported here show interesting results in that there appears to be a great deal of specificity regarding particular cells in defined areas and the synthesis of particular cytokines and proteins. These findings are very similar to our results in cultured cells [4, 5, 6], showing that the use of a cell culture model can yield meaningful data to elucidate the mechanisms that occur in PD and possibly other neurodegenerative disorders.

Continuing work has led to some consensus among scientists that inflammatory episodes [7], cytokines [24], dopaminergic cell death [25, 26], selective cell targeting [27] and disruptions of protective proteins [28], such as GDNF [29], are all involved in eventual cell death and loss of cell signaling in neurodegenerative diseases [30]. Activated microglia but not "intact resting microglia", have been postulated as culprits in neurodegeneration, and this finding might be an explanation for our observations of a selective population of cells being positive for cytokine production and protein aggregations [31]. This theme is continued in a recent report which suggests that microglial inflammation may induce dopaminergic neuronal cell death via the release of NO and cytokines and this mechanism has been seen as a possible point of intervention for therapeutic treatment of neurodegeneration [32, 33], in which microglial protective mechanisms are initiated when they are not really required, causing subsequent detrimental consequences and resultant neurodegeneration [34, 35, 36].

This current research extends our previous studies in cell culture models and again identifies the apparent specificity of the 'appearance' of particular cytokines and localization of products to particular cells and areas. Interleukin-10 is upregulated and a representative image is shown in Figure 6 possibly indicating initiation of a protective mechanism as previously reported [37]. We also hypothesize that the fluorescing cells are a distinct population that need to be identified, especially as to their role in chronic Parkinson's diseases, such that they can become a therapeutic target.

CONCLUSIONS

Our results point to a gradual decline in cellular sustainability to the extent that subsequent assaults, illnesses, inflammatory problems, or even stress, reintroduces cells into their protective role, but a role that is inevitably overcome. This gradual decline describes why Parkinson's disease is such a chronic illness [38] as only when all protective mechanisms have been overcome, does the dopaminergic neuron itself become the sole target for pro-inflammatory cytokines, protein aggregations and loss of a functional ubiquitin-proteasome recycling pathway [39, 40]. This hypothesize has been noted previously by Del Tredici and Braak [41] as a "depletion of nigrostriatal projection", and Halliday [42, 43] states that the chronic progression of the disease allows for some hope of tissue specific markers, markers that could be identified in an LPS animal model and, as Meredith *et al.* [44] reported, such models are probably better for the identification of preclinical, rather than clinical markers.

ABBREVIATIONS

LPS – lipopolysaccharide bacterial endotoxin
PD – Parkinson's disease
IL-6 – interleukin 6
TNF – Tumor necrosis factor alpha
IL-10 – interleukin 10
IFN – gamma interferon
IL-1β – interleukin 1-beta
PBS – Phosphate buffered saline
GDNF – glial cell line-derived neurotrophic factor
NOS – nitric oxide synthase
iNOS – inducible nitric oxide synthase
IL-4 – interleukin 4

REFERENCES

1. Reale, M., Iarlori, C., Thomas, A., Gambi, D., Perfetti, B., Di Nicola, M. and Onofrj, M. 2009, Brain Behav. Immun., 23, 55.
2. Hirsch, E. C. and Hunot, S. 2009, Lancet Neurol., 8, 382.

3. Hisanaga, K., Asagi, M., Itoyama, Y. and Iwasaki, Y. 2001, Arch. Neurol., 58, 1580.
4. Bick, R. J., Poindexter, B. J., Kott, M. M., Liang Y. A., Dinh, K., Kaur, B., Bick, D. L., Doursout, M. F. and Schiess, M. C. 2008, Brain Res., 1217, 203.
5. Dinh, K., Poindexter, B. J., Barnes, J. L., Schiess, M. C. and Bick, R. J. 2009, Cytokine, 45, 179.
6. Schiess, M. C., Barnes, J., Poindexter, B. J., Dinh K. and Bick, R. J. 2010, BMC Neurosci., 29, 151.
7. Arai, H., Furuya, T., Mizuno, Y. and Mochizuki, H. 2006, Histol. Histopathol., 21, 673.
8. Semmler, A., Okulla, T., Sastre, M., Dimitrescu-Ozimek, L. and Heneka, M. T. 2005, J. Chem. Neuroanat., 30, 144.
9. Chalimoniuk, M., Stolecka, A., Ziemińska, E., Stepień, A., Langfort, J. and Strosznajder, J. B. 2009, J. Neurochem., 110, 307.
10. Zhou, L. and Zhu D. Y. 2009, Nitric Oxide, 20, 223.
11. Hoang, T., Choi, D. K., Nagai, M., Wu, D. C, Nagata, T., Prou, D., Wilson, G. L., Vila, M., Jackson-Lewis, V., Dawson, V. L., Dawson, T. M., Chesselet, M. F. and Przedborski, S. 2009, Free Radic. Biol. Med., 1, 1049.
12. Kaur, C. and Ling, E. A. 2008, Curr. Neurovasc. Res., 5, 71.
13. Qian, L., Flood, P. M. and Hong, J. S. 2010. J. Neural. Transm., 117, 971.
14. Stamatovic, S. M, Keep, R. F. and Andjelkovic, A. V. 2008. Curr. Neuropharmacol., 6, 179.
15. Reynolds, A. D., Banerjee, R., Liu, J., Gendelman, H. E. and Morley, R. L. 2007, J. Leuk. Biol., 82, 1083.
16. Panaro, M. A. and Cianciulli A. 2012, Curr. Pharm. Des., 18, 200.
17. Akundi, R. S., Huang, Z., Eason, J., Pandya, J. D., Cass, W. A., Sullivan, P. G. and Bueler, H. 2011, PLoS One, 6, 1.
18. Paxinos, G. and Watson, C. 1997, The Rat Brain in Stereotaxic Coordinates, 4th ed., Academic Press: New York, NY.
19. Poindexter, B. J., Pereira-Smith, O. M., Smith, J. R., Buja, L. M. and Bick, R. J. 2002, Microsc. Anal., 16, 21.
20. Merritt, T. M., Bick, R., Poindexter, B. J. and Hecht, J. T. 2007, Amer. J. Pathol., 170, 293.
21. Doursout, M. F., Oguchi, T., Fischer, U. M., Liang, Y., Chelly, B., Hartley, C. J. and Chelly, J. E. 2008, Shock, 29, 692.
22. Forsyth, C. B., Shannon, K. M., Kordower, J. H., Voigt, R. M., Shaikh, M., Jaglin, J. A., Estes, J. D., Dodiya, H. B. and Keahavarzian, A. 2011, PLoS One, 2, e28032.
23. Theodore, S., Cao, S., McLean, P. J. and Standaert, D. G. 2008, J. Neuropathol. Exp. Neurol., 67, 1149.
24. Choi, D. K., Koppula, S., Choi, M. and Suk, K. 2010, Expert Opin. Ther. Pat., 20, 1531.
25. Chung, C. Y., Koprich, J. B., Siddiqi, H. and Isacson O. 2009, J. Neurosci., 29, 3365.
26. Saijo, K., Winner, B., Carson, C. T., Collier, J. G., Boyer, L., Rosenfeld, M. G., Gage, F. H. and Glass, C. K. 2009, Cell, 137, 47.
27. Nagatsu, T., Mogi, M., Ichinsoe, H. and Togari, A. 2000, J. Neural. Transm. Suppl., 60, 277.
28. Pieper, H. C., Evert, B. O., Kaut, O., Riederer, P. F., Waha, A. and Wüllner, U. 2008, Neurobiol. Dis., 32, 521.
29. Du, Y., Li, X., Yang, D., Zhang, X., Chen, S., Huang, K. and Le, W. 2008, Exp. Biol. Med., 233, 881.
30. Hirsch, E. C. 2007, Parkinsonism. Relat. Disord., 13(Suppl. 3), S332.
31. Sui, Y., Stanic, D., Tomas, D., Jarrott, B. and Horne, M. K. 2009, Neurosci. Lett., 460, 121.
32. Lipton, S. A., Gu, Z. and Nakamura, T. 2007, Int. Rev. Neurobiol., 82, 1.
33. Delgado, M. and Ganea, D. 2003, FASEB J., 17, 944.
34. Banati, R. B., Gehrmann, J., Schubert, P. and Kreutzberg, G. W. 1993, Glia, 7, 111.
35. Block, M. L., Zecca, L. and Hong, J. S. 2007, Nat. Rev. Neurosci., 8, 57.
36. Sawada, M. 2009, Parkinson Relat. Dis., 15, S39.
37. Arimoto, T., Choi, D. Y., Lux, X., Liu, M., Nguyen, X. V., Zheng, N., Stewart, C. A., Kim, H. C. and Bing, G. 2007, Neurobiol. Aging, 28, 894.
38. Olanow, C. W., Kieburtz, K. and Scapira, A. H. 2008, Ann. Neurol., 64(Suppl. 2):S101-110.

39. Frank-Cannon, T. C., Alto, L. T., McAlpine, F. E. and Tansey, M. G. 2009, Mol. Neurodegener., 16, 47.
40. Huang, Q. and Figueiredo-Pereira, M. E. 2010, Apoptosis, 15, 1292.
41. Del Tredici, K. and Braak, H. 2008, Acta Neuropathol., 115, 379.
42. Halliday, G., Del Tredici, K. and Braak, H. 2006, J. Neural. Transm. Suppl., 70, 99.
43. Halliday, G. 2008, Acta Neuropathol., 114, 377.
44. Meredith, G. E., Sonsalla, P. and Chesselet, M. F. 2008, Acta Neuropathol., 2008, 115, 385.